Topological Analysis of Tendon-Driven Manipulators

by J.J. Lee and L.W. Tsai

TECHNICAL RESEARCH REPORT

SYSTEMS RESEARCH CENTER

Supported by the National Science Foundation Engineering Research Center Program (NSFD CD 8803012), Industry and the University

TR 90-55

TECHNICAL
RESEARCH
REPORT

SYSTEMS
RESEARCH
CENTER

*Supported by the
National Science Foundation
Engineering Research Center
Program (NSFD CD 8803012)
and Industry*

Research support for this
report has been provided by
DOE

Topological Analysis of Tendon-Driven Manipulators

by J.J. *Lee and L.W. Tsai*

SRC TR 90-55

Topological Analysis of Tendon-Driven Manipulators

Jyh-Jone Lee
Graduate Research Assistant

Lung-Wen Tsai
Professor

Department Of Mechanical Engineering and
Systems Research Center
The University of Maryland
College Park, MD 20742

Abstract

This paper investigates the effect of tendon routing on kinematic and static force transmission associated with tendon-driven manipulators. The transmission characteristics can be described by the velocity and/or force ellipsoid. We have shown that the effect of tendon routing can be characterized by a condition number and the direction of a homogeneous solution. The condition number is defined as the ratio of the maximum to the minimum singular value of the structure matrix and the homogeneous solution is the set of tendon forces that results in no net joint torques. A methodology for calculating maximum tensions in a tendon-driven manipulator has been developed. We have also shown that among the various tendon routings in three-DOF manipulators, the one with an isotropic transmission ellipsoid possesses minimal maximum tendon force.

1. Introduction

Tendon has been widely used for power transmission in the field of robot manipulators. The advantage of using tendons for power transmission is that it allows actuators to be installed at the base and, therefore, reduces the size and inertia of the system. For examples both UTAH-MIT (Jacobsen et al., 1984) and Stanford-JPL (Salisbury, 1982) Hands are tendon-driven manipulators.

A special characteristic associated with tendon-driven manipulators is that tendon can only exert tension. In other words, force can only be transmitted from an actuator to the joints in a unidirectional sense. This imposes certain constraints on the arrangement of tendon routings (Morecki et al., 1980; Lee and Tsai, 1990). For examples: (a) An n-DOF (Degree-of-Freedom) manipulator requires at least (n+1) tendons; (b) the joint angles are related to tendon displacements by a structure matrix; (c) the rank of the structure matrix is equal to the number of DOF; (d) there must be a minimum of two non-zero elements and a minimum of one sign change in each row of the structure matrix; and (e) if m is the number of tendons, then there exists an (m-n) dimensional homogeneous solution and all the elements in the homogeneous solution must be positive.

Based on the above constraints, we can ask ourselves the following questions. For a given number of DOF, how many different ways of tendon routings are admissible? And if we know the answer, what is the best routing? In a prior work (Lee and Tsai, 1990), we established a methodology for the enumeration of admissible tendon routing for manipulators having pseudo-triangular structure matrix. All the admissible kinematic structures with up to six degrees of freedom were enumerated. In this paper, the kinemtic and static force transmission characteristics associated with tendon-driven manipulators will be investigated and the structural differences among various tendon routings wil be compared.

The theory of differential geometry has been used for the study of force and/or motion transformation between the joint space and end-effector space in an open-loop manipulator (Asada and Granito, 1985; Yoshikawa, 1985; and Ghosal and Roth, 1987). In what follows we shall extend the theory to the analysis of force and/or motion transformation between the actuator space and joint space in tendon-driven manipulators. First, we will show that a tendon-driven manipulator can be characterized by the condition number, defined as the ratio of the maximum singular value to the minimum singular value of the structure matrix, and the direction of its homogeneous solution to the structure matrix. Then, we will define an index for measuring the goodness of tendon routings and show that isotropic transformation between the actuator space and joint space can be achieved for certain types of routings. Finally, we will demonstrate a method for resolving the maximum tension required to produce a set of desired joint torques.

2. Principle of Operation

It has been shown by Tsai and Lee (1989), that the kinematic structure of spatial tendon-driven manipulators can be represented by a planar schematic from which the transformation matrix relating tendon displacements to the joint angles can be derived systematically.

Specifically, for an n-DOF manipulator with m open-ended control tendons, $m \geq n + 1$, the mapping from joint rate, $\underline{\dot{\theta}}$, to tendon linear velocity, $\underline{\dot{S}}$, can be written as:

$$\underline{\dot{S}} = A\,\underline{\dot{\theta}} \tag{1.a}$$

where A is an m x n matrix. If all pulleys pivoted about one joint axis are of the same radius, then the matrix A can be decomposed into a product of two matrices:

$$A = B\,R \tag{1.b}$$

where R is an n x n diagonal matrix whose diagonal elements are the radii of the pulleys, and matrix B whose elements consist of -1, 0, and +1 is an m x n matrix describing the routing of tendons.

As to the force transformation, it has been shown that the resultant torque, $\underline{\tau}$, about the joint axes in the equivalent open-loop chain, are related to tendon force $\underline{f}$, by:

$$\underline{\tau} = A^T \underline{f} \tag{2.a}$$

or

$$\underline{\tau} = R^T B^T \underline{f}, \text{ provided } A = BR \tag{2.b}$$

Equations (1) and (2) describe the basic relationship necessary for the kinematic and force control of open-ended tendon-driven manipulators. In the velocity domain, once the joint rates are known, linear velocities of the tendons are uniquely determined. Conversely, linear velocities of the tendons can not be specified independently. The attainable tendon velocities are contained in an n-dimensional column space of A. In the force domain, once tensions in the tendons are specified, resultant torques about the joint axes are uniquely determined. Conversely, for a given set of joint torques, Eq. (2) constitutes a set of simultaneous equations in which the number of unknows, m, is greater than the number of equations, n. When m = n + 1, the solution $\underline{f}$ can be generally expressed as the summation of a particular solution and a homogeneous solution as shown below:

$$\underline{f} = (R^T B^T)^+ \underline{\tau} + \lambda \underline{f}_h \tag{3}$$

where $(\ )^+ = \{(\ )^T[()\ ()^T]^{-1}\}$ (Strang, 1980) represents the pseudo-inverse of (), $\underline{f}_h$ lies in the null space of the structure matrix B^T, and λ is an arbitrary constant. The vector $\underline{f}_h$ represents a set of tendon forces which results in no net joint torques. The components of the homogeneous solution must be of the same sign. Thus by adjusting the constant λ, positive tension can be maintained in every tendon.

The structure matrix B^T is of primary importance in determining the characteristics of a manipulator, since R is a non-singlular square matrix which does not affect the generic property of a manipulator. In what follows, we shall consider those tendon-driven manipulators with the number of tendons, m, greater than the number of DOF, n, by one. Also, for the sake of clarity, we shall assume R is an identity matrix so that manipulators are normalized in radius uniformity. We will use the case n = 2 and m = 3 to develop the concept throughout this paper.

3. Transmission Ellipsoid

The planar schematic of a two-DOF tendon-driven manipulator with three control tendons is shown in Fig. 1. Defining the positive axes of rotation about the joints to be pointing out of the paper, we can write down Eq. (2.b) as:

$$\underline{\tau} = B^T \underline{f} \tag{4}$$

where $\underline{\tau} = [\tau_1 \ \tau_2]^T$, $\underline{f} = [f_1 \ f_2 \ f_3]^T$ and $B^T = \begin{bmatrix} -1 & 1 & 0 \\ -1 & -1 & 1 \end{bmatrix}$

In this notation, the joints are numbered sequentially from the distal end. When there is no joint torque requirement, tendon forces are given by the homogeneous solution, $\underline{f}_h = \lambda \ [1 \ 1 \ 2]^T$ and not much more can be said about it. One effective method is to compare tendon forces required to achieve a unity joint torque in all directions, that is,

$$\underline{\tau}^T \ \underline{\tau} = 1 \tag{5}$$

For a two-DOF system, Eq. (5) represents a circle in the joint-torque space as shown in Fig. 2(a). Substituting Eq. (4) into (5), we obtain:

$$\underline{f}^T B B^T \underline{f} = 1 \tag{6}$$

Since matrix B^T is of rank two, the quantity (BB^T) is a symmetric 3 x 3 matrix of rank two. Therefore, Eq. (6) describes a cylinder with its elements oblique to the axes in the tendon-force space as shown in Fig. 2(b). The principal axes of this force ellipsoid coinside with the eigenvectors of (BB^T) and the lengths of its principal axes are equal to the reciprocals of the square roots of the eigenvalues. Since (BB^T) is a symmetic 3 x 3 matrix of rank two, it always has an eigenvalue of zero magnitude which results in a principal axis of infinite length. Physically, this axis defines the direction of the homogeneous solution of Eq.(4).

Force Ellipsoid

The force ellipsoid shown in Fig. 2(b) is a useful tool for visualizing force transmission characteristics. From geometric point of view, each element of the cylindrical surface in the tendon-force space maps onto a point in the joint-torque space. This implies that tendon forces can be propotionally increased along the direction of its homogeneous solution without affecting the resultant joint torques. If the direction of the homegeneous solution is not contained in the first quadrant, then increasing tendon forces along the longitudinal direction of the cylindrical surface will result in some negative tensions. Hence, all components of the homogeneous solution must be positive.

Velocity Ellipsoid

Similar to force ellipsoid, we can also depict a velocity ellipsoid to visualize the velocity transmission characteristics. Velocity in the joint space can be mapped into tendon space via Eq. (1). For a unity R, Eq. (1), can be written as follows:

$$\underline{\dot{S}} = B\,\underline{\dot{\theta}} \tag{7}$$

Given $\underline{\dot{S}}$, the solution of $\underline{\dot{\theta}}$ can be derived from the least-square method, since the number of equations is greater than the number of unknowns. Taking the left general inverse of B, Eq. (7) yields:

$$\underline{\dot{\theta}} = {}^{l}B^{+}\ \underline{\dot{S}} \tag{8}$$

where ${}^{l}B^{+}$ is defined as $[(B^TB)^{-1}\ B^T]$. Restraining $\underline{\dot{\theta}}$ with unit speed condition, we can have:

$$\underline{\dot{\theta}}^T\ \underline{\dot{\theta}} = \underline{\dot{S}}^T\ ({}^{l}B^{+})^T\ {}^{l}B^{+}\ \underline{\dot{S}} = 1 \tag{9}$$

The quantity $({}^{l}B^{+})^T\ {}^{l}B^{+}$ is a symmetric 3 x 3 matrix of rank two. Therefore, the velocity vector $\underline{\dot{S}}$ depicts an ellipse as shown in Fig. 2(c).

Another quick way to depict the velocity ellipsoid is to apply the duality property of force and velocity. The principal axes of the velocity and force ellipsoids coincide, and the lengths of the axes are inversly proportional to one another. Hence, principal axes of the velocity ellipsoid shown in Fig. 2(c) are oriented in the same directions as those of the force ellipsoid shown in Fig. 2(b), and its lengths are the reciprocals of the force ellipsoid. Note that one of the axis (corresponding to the homogeneous solution) in the force ellipsoid is infinitely long; therefore, the length of the corresponding axis in the velocity ellipsoid is zero. Also note that although $\underline{\dot{S}}$ has one fewer DOF than $\underline{f}$, $\underline{\dot{S}}$ still implicitily describes an ellipsoid with a degenerate axis of zero length.

4. The Isotropy of the Transmission Ellipsoid

It is well known that velocity transformation between the joint space and end-effector space of a manipulator can be characterized by the Jacobian matrix J. The condition number of the Jacobian matrix has been used as a quality index for measuring the performance of a manipulator. The condition number is defined as the product of the norms of J and J^{-1} (Strang, 1980). It can also be used as an indicator for measuring the shape of the transmission ellipsoid. When the condition number is equal to one, we call the mapping isotropic. Isotropic transmission has advantageous properties as discussed by Salisbury and Craig (1982) and Gosselin and Angeles (1988). For tendon-driven manipulators, the force transmission ellipsoid formed by the structure matrix B^T has an axis of infinite length. Therefore, traditional definition for the condition number can no longer be used. In this paper, the condition number for the structure matrix is defined as:

$$\mathrm{cond}(B^T) = \frac{\text{max. singular value of } B^T}{\text{min. singular value of } B^T} \tag{10}$$

From geometric point of view, this condition number measures the shape of the cross section perpendicular to the longitudinal axis of the cylinder. When the value is close to one, the shape of the cross section approaches to a circle. The application of this index can be explained as follows. The cylinder intersects with the f_2-f_3, f_3-f_1, and f_1-f_2 planes in three curves l_1, l_2, and l_3, respectively, as shown in Fig. 2(b). Physically, these intersecting curves are the loci of minimal tendon forces required to produce a unity joint torque in all directions as shown in Fig. 2(a). Therefore, we can readily see that the shape of the cross section and the direction of the longitudinal axis will have some dominant effect on the location of the curves. An ideal condition would be for the interesecting curves, l_1, l_2, and

l_3 to be symmetrically located with respect to the origin. For the ideal condition to happen, the cylinder will have a circular cross section and the longitudinal axis must intersect all the coordinate axes at equal angles.

From the above discussion, we can conclude that the direction of the longitudinal axis plays an important role in the distribution of tendon forces. The more the longitudinal axis is skewed, i.e the components of the vector are in an odd proportion, the larger the difference in tensions will occur. This will result in a severe antagonism among the tendons and greatly reduce the efficiency of the system. Therefore, it is desirable to have the longitudinal axis of the cylinder pointed as closely toward the direction which makes equal angles with all the coordinate axes as possible. We shall call the vector which makes equal angles with all the coordinate axes as the isotropic vector. Define

$$\theta^* = \cos^{-1} (\underline{U} \cdot \underline{I}_s) \tag{11}$$

where $\underline{U}$ is a unit vector defined along the longitutinal axis of the cylinder and $\underline{I}_s$ is the unit isotropic vector. Then, the angle θ^* can be used to indicate the closeness of the longitudinal axis to the isotropic vector. In the three-dimensional space, the unit isotropic vector is given by $[1/\sqrt{3}\ 1/\sqrt{3}\ 1/\sqrt{3}]^T$. In an n-dimensional space, it is given by $[1/\sqrt{n}\ 1/\sqrt{n}\ \ldots\ 1/\sqrt{n}]^T$.

We define an isotropic transmission ellipsoid as one which has a unit condition number and the isotropic vector as the direction of the homogeneous solution.

5. Maximum Tendon Force

To compute tendon forces, we first obtain a particular solution to

Eq.(3), then the homogeneous solution multiplied by a constant λ is added onto the particular solution. The constant λ should be chosen such that all the tendons are under tension. The result is exactly the same as finding the intersection of the force ellipsoid with its coordinate planes, i.e., solving l_1, l_2, and l_3 in terms of joint torques. This procedure can be accomplished by substituting the equations of planes $f_i = 0$ $(i=1,2,3)$ into Eq.(4), and then solving for f_j $(j=1,2,3;\ j\neq i)$. For the 2-DOF example, substituting $f_1 = 0$ into Eq. (4), we obtain l_1 in parametric form as

$$\begin{cases} f_2 = \tau_1 \\ f_3 = \tau_1 + \tau_2 \end{cases} \qquad (12.a)$$

where τ_1 and τ_2 are subject to Eq. (5).

Similarly, substituting $f_2 = 0$ into Eq. (4), we obtain l_2 as

$$\begin{cases} f_1 = -\tau_1 \\ f_3 = -\tau_1 + \tau_2 \end{cases} \qquad (12.b)$$

Substituting $f_3 = 0$ into Eq. (4), we obtain l_3 as

$$\begin{cases} f_1 = (-\tau_1-\tau_2)/2 \\ f_2 = (\tau_1-\tau_2)/2 \end{cases} \qquad (12.c)$$

The maximum value of f_j can be found using Cauchy-Schwarz inequality formula. For example, applying Cauchy-Schwarz inequality to Eq. (12.a), we obtain

$$f_2^2 = \tau_1^2 \leq (1^2 + 0^2)(\tau_1^2 + \tau_2^2)$$

or

$$f_2 \leq 1$$

Applying Cauchy-Schwarz inequality to Eq. (12.c), we obtain

$$f_2^2 = (\tau_1/2 - \tau_2/2) \le (1/2^2 + 1/2^2)(\tau_1^2 + \tau_2^2)$$

or

$$f_2 \le 1/\sqrt{2}$$

Hence, tendon f_2 has an extreme value of 1. Similarly, extreme values of f_1 and f_3 can be found.

The above procedure can be extended to n-DOF manipulators. For an n-DOF manipulator, there are (n+1) hyperplanes with which the (n+1)-dimensional force ellipsoid may intersect. The equations of the hyperplanes can be represented as

$$f_i = 0, \qquad i=1,2,\ldots,n+1 \tag{13}$$

Substituting Eq. (13) into (2), we obtain:

$$\underline{\tau} = B_i^T \, \underline{f}^i \tag{14}$$

where B_i^T is the matrix obtained by deleting the i^{th} column from B^T and $\underline{f}^i$ is the column matrix obtained by deleting the i^{th} element of $\underline{f}$.

For each i, Eq. (14) denotes n linear equations in n unknowns. Hence, $\underline{f}^i$ can be solved by inverting B_i^T or using Crammer's rule. The j^{th} element, f_j, can then be written as:

$$f_j = \frac{(-1)^s \left| \underline{\tau} \; B_{ij}^T \right|}{\left| B_i^T \right|} \tag{15}$$

where

$$\begin{cases} s = j - 1, & \text{if } i > j \\ s = j, & \text{if } i < j \end{cases}$$

and where $i=1,2,\ \ldots,\ n+1$, $j=1,2,\ldots,\ n+1$, $j \neq i$, B_{ij} represents the matrix obtained by deleting the i^{th} and j^{th} columns of B^T, and where $|\ (\ )\ |$ represents the determinent of ( ). There are $n(n+1)$ such equations. For each equation, an extreme value of tendon force can be found using Cauchy-Schwarz inquality formula. Comparing these extreme values, we can differentiate the static performance among various tendon routings.

6. Application to Three-DOF Manipulators

In this section, we will apply the foregoing concept to analyzing three-DOF manipulators. For a three-DOF manipulator, there are four tendons. Therefore, to achieve a unit joint torque in all directions, joint torques describe a three-dimensional sphere while tendon forces describe a four-dimensional cylinder with an axis of infinite length. The condition number of the structure matrix measures the shape of directrix of the cylinder. Fig. 3 shows five non-isomorphic tendon-driven manipulators. For a detailed development of these non-isomorphic structures, the reader is referred to the paper by Lee and Tsai (1990). Table 1 lists the structure matrices B^T, homogeneous solution $\underline{f}_h$, condition number C, and the angle θ^* for the kinematic structures shown in Fig. 3, respectively.

Note that Fig.3 (c) represents the kinemetic structure of a finger in the Stanford-JPL hand (Salisbury, 1982). The homogeneous solution of the Stanford-JPL finger points in the isotropic direction, $\theta^* = 0$. However, its condition number is not equal to one, C = 2.618. On the other hand, the tendon routing as shown in Fig. 3(d) results in an isotropic transmission. All other kinematic structures show different extent of non-isotropy in terms of the condition number and the angle θ^*.

Table 2 lists the maximum tendon force for the structures shown in Fig. 3. To differentiate the performance difference among various structures, we can define the optimality criterion as follows:

$$\text{Objective function: } \min_{(B^T)_i \; \underline{f}} [\max (f_j)], \qquad \text{subject to } \underline{\tau}^T \underline{\tau} = 1 \tag{16}$$

where max (f_j) denotes the maximum tendon force in a given kinematic structure, and min [ ] denotes the minimal maximum-tendon-force among a set of different structures.

It can be seen that the structure shown in Fig. 3(d) requires minimal maximum-tendon-force which is two times smaller than that of the structure shown in Fig. 3(c). An additional merit of the structure shown in Fig. 3(d) is that it requires equal strength actuators and tendons. This characteristic can simplify the selection of actuators.

7. Summary

We have performed the analysis of force and velocity transmission for tendon-driven manipulators. It has been shown that the effect of routing on force/velocity transmission can be characterized by both the condition number and the direction of homogeneous solution to the structure matrix. Isotropic transmission of tendon-driven manipulators has been defined and several three-DOF kinematic structures have been used to illustrate the concept. In addition, a criterion for differentiating force transmission characteristics has been defined and a procedure for the identification of minimal maximum-tedon-force has been presented. We have shown that the kinematic structure of a three-DOF manipulator as shown in Fig. 3(d) satisfies the isotropic transmission as well as minimal maximum-tendon-force conditions. The results may offer some insight for the synthesis of tendon-driven robotic manipulators.

8. Acknowledgement

This work was supported in part by the U.S. Department of Energy under grant DEF05-88ER 13977 and in part by the NSF Engineering Research Centers program, NSF CDR 8803012. Such support does not constitute an endorsement by the supporting agencies of the views expressed in the paper.

9. References

1. Asada, H., and Cro Granito, J.A., 1985, "Kinematic and Static Characterization of Wrist and Their Optimal Design," IEEE Proc. of Intl. Conf. on Robotics and Automation, pp. 244-250.

2. Ghosal, A., and Roth, B., 1987, "Instantaneous Properties of Multi-Degree-of-Freedom Motions-Point Trajectories," Trans. of ASME, J. of Mechanisms, Transmissions and Automation in Design, Vol. 109, No.1, pp. 107-115.

3. Gosselin, C., and Angeles J., 1988, "Optimum Kinematic Design of a Planar Three-Degree-of-Freedom Parallel Manipulator," Trans. of ASME, J. of Mechanisms, Transmissions and Automation in Design, Vol. 110, No. 1, pp. 35-41.

4. Jacobsen, S.C., Wood, J.E., Knutti, D.F., and Biggers, K.B., 1984, "The Utah-MIT Dextrous Hand: Work in Progress," Intl. J. of Robotics Research, Vol. 3, No. 4, pp. 21-50.

5. Lee, J.J. and Tsai, L.W., 1990, "On the Structural Synthesis of Tendon-Driven Manipulators Having Pseudo-Triangular Structure Matrix," Intl. J. of Robotics Research, to appear.

6. Morecki, A., Busko, Z., Gasztold, H., and Jaworek, K., 1980, "Synthesis and Control of the Anthropomorphic Two-Handed Manipulator," Proc. of the 10th Intl. Symposium on Industrial Robots, Milan, Italy.

7. Salisbury, J.K., 1982, "Kinematic and Force Analysis of Articulated Hands," Dissertation, Stanford University, Mech. Engr. Dept., Stanford, CA.

8. Salisbury, J.K., and Craig, J.J., 1982, "Articulated Hands: Force Control and Kinematic Issues," Intl. J. of Robotics Research, Vol. 1, No.1, pp. 4-17.

9. Strang, G., 1980, Linear Algebra and Its Applications, Academic Press, Inc.

10. Tsai, L.W., and Lee, J.J., 1989, "Kinematic Analysis of Tendon-Driven Robotic Mechanisms Using Graph Theory," Trans. of ASME, J. of Mechanisms, Transmissions, and Automation in Design,Vol. 111, No. 1, pp. 59-65.

11. Yoshikawa, T., 1985, "Manipulability and Redundancy Control of Robotic Mechanism," IEEE Proc. of Intl. Conf. on Robotics and Automation, pp. 1004-1009.

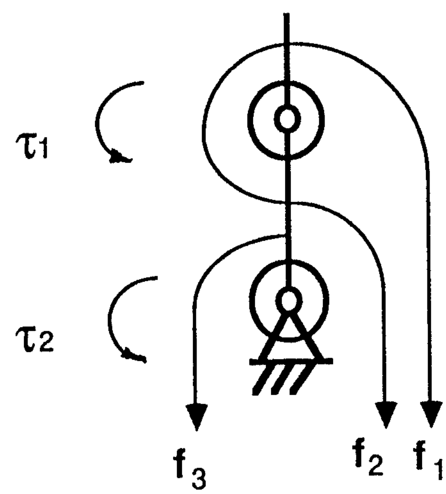

(a)

Fig. 1

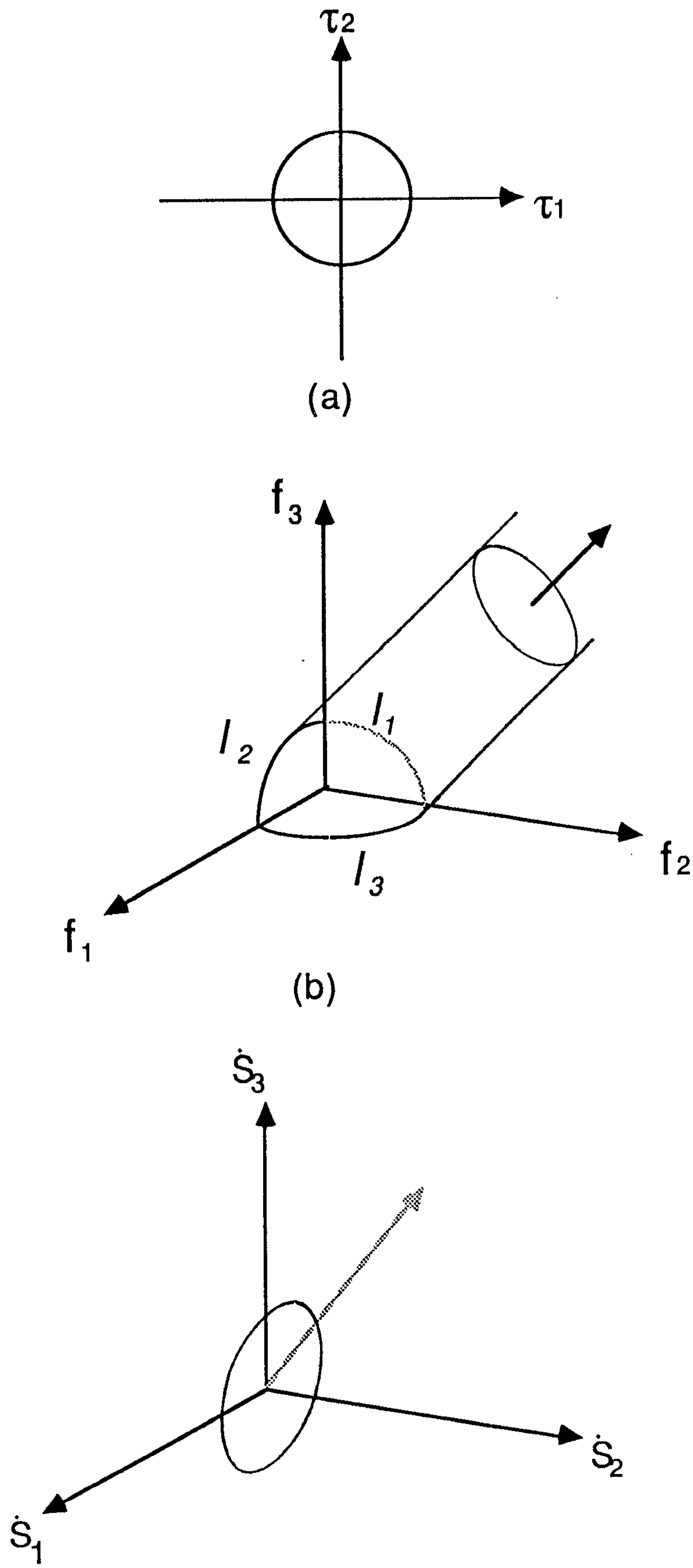

(c)

Fig. 2

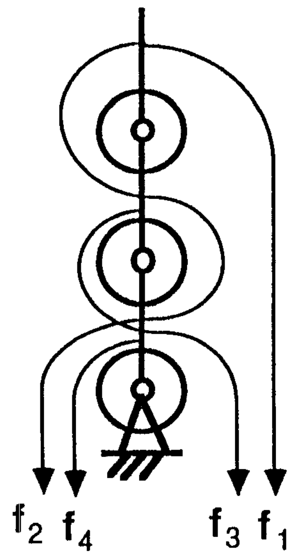

(a)

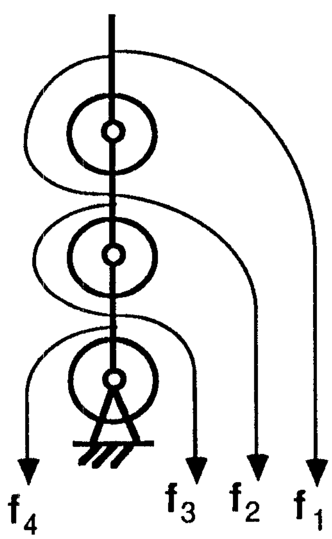

(b)

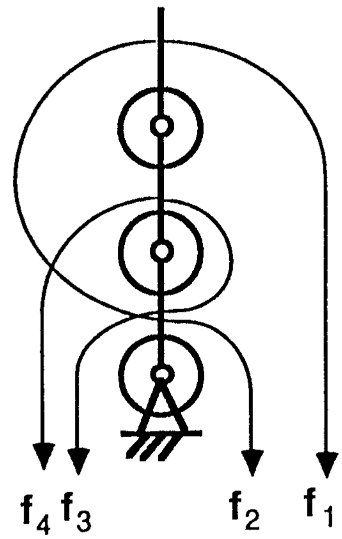

(c)

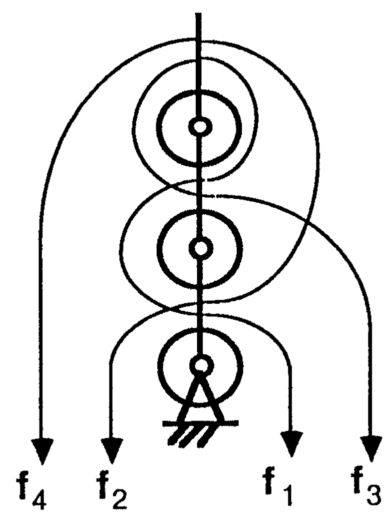

(d)

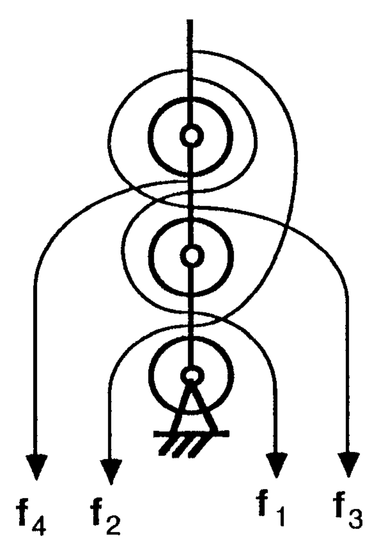

(e)

Fig. 3

Fig.3	B^T	$\underline{\mathbf{f}}_h$	c	θ^*
(a)	$\begin{bmatrix} -1 & 1 & 0 & 0 \\ -1 & -1 & 1 & 0 \\ -1 & 1 & -1 & 1 \end{bmatrix}$	$\begin{bmatrix} 1 \\ 1 \\ 2 \\ 2 \end{bmatrix}$	2.943	18.43°
(b)	$\begin{bmatrix} -1 & 1 & 0 & 0 \\ -1 & -1 & 1 & 0 \\ -1 & -1 & -1 & 1 \end{bmatrix}$	$\begin{bmatrix} 1 \\ 1 \\ 2 \\ 4 \end{bmatrix}$	1.520	31.48°
(c)	$\begin{bmatrix} -1 & 1 & 0 & 0 \\ -1 & 1 & -1 & 1 \\ -1 & -1 & 1 & 1 \end{bmatrix}$	$\begin{bmatrix} 1 \\ 1 \\ 1 \\ 1 \end{bmatrix}$	2.618	0
(d)	$\begin{bmatrix} -1 & -1 & 1 & 1 \\ 1 & -1 & -1 & 1 \\ -1 & 1 & -1 & 1 \end{bmatrix}$	$\begin{bmatrix} 1 \\ 1 \\ 1 \\ 1 \end{bmatrix}$	1	0
(e)	$\begin{bmatrix} -1 & -1 & 1 & 0 \\ 1 & -1 & -1 & 1 \\ -1 & 1 & -1 & 1 \end{bmatrix}$	$\begin{bmatrix} 1 \\ 1 \\ 2 \\ 2 \end{bmatrix}$	1.581	18.43°

Table 1

Fig.3	(a)	(b)	(c)	(d)	(e)
$\begin{bmatrix}\max(f_1)\\ \max(f_2)\\ \max(f_3)\\ \max(f_4)\end{bmatrix}$	$\begin{bmatrix}1\\ \sqrt{3/2}\\ \sqrt{2}\\ \sqrt{6}\end{bmatrix}$	$\begin{bmatrix}1\\ 1\\ \sqrt{2}\\ \sqrt{6}\end{bmatrix}$	$\begin{bmatrix}\sqrt{3/2}\\ \sqrt{3/2}\\ \sqrt{2}\\ \sqrt{2}\end{bmatrix}$	$\begin{bmatrix}1/\sqrt{2}\\ 1/\sqrt{2}\\ 1/\sqrt{2}\\ 1/\sqrt{2}\end{bmatrix}$	$\begin{bmatrix}1/\sqrt{2}\\ 1/\sqrt{2}\\ \sqrt{3/2}\\ \sqrt{2}\end{bmatrix}$
$\max(f_j)$	f_4	f_4	$f_3 = f_4$	$f_1 = f_2$ $= f_3 = f_4$	f_4

Table 2